Central European Journal of Energetic Materials
ISSN 1733-7178; e-ISSN 2353-1843

Cent. Eur. J. Energ. Mater. 2020, *17*(2): 262-279; DOI 10.22211/cejem/124073
Article is available in PDF-format, in colour, at:
http://www.wydawnictwa.ipo.waw.pl/cejem/Vol-17-Number2-2020/CEJEM_01086.pdf

Research paper

Study on the Thermal Stability and Decomposition Kinetics of Polypropylene Glycol – Glycidyl Azide Polymer – Polypropylene Glycol (PPG-GAP-PPG) as a Novel Triblock Copolymer Binder

Fahimeh Ghoroghchian, Yadollah Bayat*, Fatemeh Abrishami

Department of Chemistry and Chemical Engineering, Malek Asthar Univeristy of Technology, P.O. Box 16765-3454, Tehran, Iran
**E-mail:* y_bayat@mut.ac.ir

Abstract: In this study, the novel energetic triblock copolymer of polypropylene glycol- glycidyl azide polymer- polypropylene glycol (PPG-GAP-PPG) (M_n = 1419 g·mol^{-1}) was synthesized by cationic ring-opening polymerization of propylene oxide using low molecular weight glycidyl azide polymer (GAP) (M_n = 1006 g·mol^{-1}) as the initiator and boron trifluoride etherate (BF_3·OEt_2) as the catalyst. The synthesized GAP and triblock copolymer were characterized by Fourier-transform infrared (FT-IR) spectroscopy, gel permeation chromatography (GPC), and nuclear magnetic resonance spectroscopy (^{1}H and ^{13}C NMR). The thermal stability of the triblock copolymer PPG-GAP-PPG was studied by differential scanning calorimetry (DSC) and thermogravimetry (TG). The DSC results showed that the glass transition temperature (T_g) of the triblock copolymer (T_g = −63 °C) was lower than that of neat low molecular weight GAP (T_g = −53 °C). Furthermore, the results indicated that this triblock copolymer is more stable than GAP. The influence of heating rate (10, 20, 30 and 40 °C·min^{-1}) illustrated that increasing the heating rate results in an increase in the triblock copolymer's decomposition temperature. Non-isothermal methods, proposed by ASTM E698, Flynn-Wall-Ozawa (FWO) and Kissinger, were used to calculate the kinetic parameters, such as activation energy and frequenc factor, for the thermal decomposition of the triblock copolymer PPG-GAP-PPG, using the DSC-DTG

data. The activation energies calculated by the FWO and ASTM E698 methods were 124.610 and 126.13 kJ·mol^{-1}, respectively.

Keywords: glycidyl azide polymer, polypropylene glycol, triblock copolymer, thermal stability, non-isothermal kinetics

1 Introduction

A binder is a polymeric system that keeps a propellant's components together, and determines the mechanical properties of the propellant and the formulation of the energetic material. Two main groups of a binders are neutral binders, such as hydroxyl-terminated polybutadiene (HTPB), polyethylene glycol (PEG), polypropylene glycol (PPG), polycaprolactone (PCL) and polybutadiene acrylic acid-acrylonitrile (PBAN), and energetic binders, such as glycidyl azide polymer (GAP), polyglycidyl nitrate (PGN) and nitro hydroxyl-terminated polybutadiene (NHTPB).

Neutral binders have a loading capacity for solids as well as low energy content in the propellant system. An appropriate polymeric binder can improve the mechanical and thermal properties of a propellant and control the propellant's safety when it is exposed to crucial situations, such as variations in temperature and pressure [1-3].

Glycidyl azide polymer (GAP), with its highly energetic azide group, is appropriate as a propellant binder and plasticizing agent due to its positive heat of formation (+957 kJ·kg^{-1}), oxygen balance (–121.1%), and compatibility with highly energetic oxidizers [4-7]. It can also produce low pollution, chlorine-free, propellants with ammonium nitrate, increasing the burning rate and specific impulse of the propellant systems [8-10]. Moreover, it can be cured easily with isocyanate curing agents to create polyurethane networks because of its hydroxyl end groups. The mechanical and thermal properties of GAP are not good enough to be used in binder systems. For instance, the glass transition temperature (T_g) of GAP (–45 °C) is higher than some neutral binders such as HTPB (–75 °C) [11], polytetrahydrofuran (PTHF) (–70 °C) [12] and PCL (–60 °C) [13]. The high T_g of GAP restricts its mobility and flexibility and limits its processability. The flexibility will affect the mechanical properties such as modulus, strength, and elongation of this energetic binder in the propellant.

Copolymerization of GAP with neutral binders with a flexible polymeric backbone can improve its mechanical and thermal properties. For this purpose, GAP-based copolymers have been synthesized using polyethylene glycol (PEG) with a higher glass transition temperature (T_g = –50.28 °C) [14].

Copolymerization of polycaprolactone (PCL) with GAP was reported by Bayat *et al.* [13] for which DSC analysis indicated a T_g of –54 °C. Ring opening of the seven-membered ring of caprolactone needs high energy and was carried out at 100 °C. In addition, the copolymers of GAP with hydroxy-terminated polybutadiene (HTPB), polybisazidomethyloxetane (PolyBAMO), and polytetrahydrofuran (PTHF) have been synthesized by other researchers and the T_g values of these copolymers were reported as –64, –35 and –60 °C, respectively. According to these studies, the thermal stability of copolymers with HTPB, PTHF and PolyBAMO is higher (or greater) than the GAP homopolymer [15-20].

Because of the secondary hydroxyl groups of GAP, its elastomers suffer from a limited selection of curing agents, poor curing conditions, and poor mechanical properties. Consequently producing primary hydroxyl groups by copolymerization can improve the mechanical properties of polyurethane based GAP.

Polypropylene glycol (PPG) has a flexible ether segment, with acceptable mechanical and thermal properties. The T_g of PPG (–70 °C) is lower than that for GAP (–45 °C). On the other hand, the elongation at fracture of PPG is 139-1000% [21]. The presence of oxygen in the repeating unit of PPG can improve the burning rate of composite propellants. Propylene oxide (PO) is also an inexpensive and readily available monomer. Therefore, the mechanical properties and T_g of GAP can be improved by copolymerization of GAP with PO. Thus, copolymerization of GAP as the macroinitiator with PO as a monomer, via a cationic ring-opening polymerization, can improve the mechanical and thermal properties of GAP [22-27].

We report here the synthesis of the triblock copolymer of polypropylene glycol – glycidyl azide polymer – polypropylene glycol (PPG-GAP-PPG). Subsequently, the kinetics parameters, such as activation energy, were quantified through the Flynn-Wall-Ozawa (FWO) and Kissinger isoconversional methods under nonisothermal conditions [28-30].

2 Materials and Methods

Dimethylformamide (DMF), boron trifluoride diethyl etherate ($BF_3 \cdot OEt_2$), sodium azide (NaN_3) and epichlorohydrin were purchased from Sigma-Aldrich. Propylene oxide (PO), 1,4-butanediol (BDO), dichloromethane and anhydrous sodium sulfate were purchased from Merck.

The Fourier transform infrared (FT-IR) spectra were measured using a Bruker Equinox 55. A Bruker model was used to record ^1H and ^{13}C NMR spectra.

$CDCl_3$ was used as the solvent and TMS as an internal standard, operating at 500 MHz. Gel Permeation Chromatography (GPC) was performed using THF as the solvent. DSC NETZSCH 200F3 model under an N_2 atmosphere and a heating rate of 10 °C·min^{-1}, from −100 to 25 °C, was used to determine the T_g values.

2.1 Synthesis of poly(epichlorohydrin) (PECH)

A 250 mL three-necked flask equipped with a magnetic stir bar, dropping funnel, and thermometer was charged with BDO as a polymerization reaction initiator (4 g, 44.2 mmol), dried dichloromethane (75 mL) and $BF_3{\cdot}OEt_2$ (1 mL), and was stirred at room temperature for 30 min. Epichlorohydrin (37 g, 386 mmol) was then added dropwise over a period of 6 h at 0 °C under a nitrogen atmosphere. The reaction mixture was stirred overnight at room temperature. Afterwards, distilled water (2 mL) was added to terminate the polymerization reaction. The mixture was extracted with dichloromethane (90 mL) and then washed with water (3 × 50 mL) to a neutral pH. The organic layer was dried over anhydrous sodium sulfate, and the dichloromethane was removed under vacuum. A colorless viscose liquid was obtained in 89% yield:

– **FT-IR:** 3380, 2845, 1190, 748 cm^{-1},
– **^{1}H NMR** ($CDCl_3$, ppm), *δ:* 1.5, 3.4, 3.6, 3.8,
– **^{13}C NMR** ($CDCl_3$, ppm), *δ*: 44, 70, 80 [28].

2.2 Synthesis of low molecular weight GAP

A 250 mL two-necked flask equipped with a magnetic stir bar, condenser, and thermometer was charged with polyepichlorohydrin (30 g), and DMF (150 mL). It was heated up to 60 °C and then sodium azide (30 g, 412 mmol) was added slowly. The azidation reaction was continued overnight at 90-110 °C under a nitrogen atmosphere. After cooling the mixture to room temperature, the unreacted sodium azide was filtered off. The reaction mixture was diluted with dichloromethane (50 mL) and washed with water (4 × 50 mL). The organic layer containing GAP and dichloromethane was dried over anhydrous sodium sulfate, and the dichloromethane was removed under vacuum. GAP (25 g, 83% yield) was obtained:

– **FT-IR**: 3400, 2880, 2100, 1100 cm^{-1},
– **GPC** analysis: M_w = 1036 g·mol^{-1}, M_n = 1006 g·mol^{-1}, PDI = 1.2,
– **^{1}H NMR** ($CDCl_3$, ppm), *δ*: 1.62, 3.35, 3.58-3.98,
– **^{13}C NMR** ($CDCl_3$, ppm), *δ*: 52, 70, 80.

2.3 Synthesis of the triblock copolymer of PPG-GAP-PPG

A 100 mL three-necked flask equipped with a magnetic stir bar, condenser, dropping funnel and thermometer was charged with GAP (15 g, 13.6 mmol, M_n = 1100) and dried dichloromethane (50 mL). $BF_3{\cdot}OEt_2$ (0.2 mL, 13 mmol) was then added dropwise at 0-5 °C. Afterwards, PO (28.6 mL, 409 mmol) was added dropwise during 6 h. The reaction mixture was stirred overnight at room temperature under a nitrogen atmosphere. It was quenched by adding distilled water (10 mL).The organic layer was then washed with water (3 × 50 mL) and dried over sodium sulfate. The solvent was removed under vacuum and 23 g (66% yield) of PPG-GAP-PPG was obtained:

- **FT-IR**: 3416, 2927, 2874, 2103, 1281, 1107 cm^{-1},
- **GPC** analysis: M_w = 2307 $g{\cdot}mol^{-1}$, M_n = 1419 $g{\cdot}mol^{-1}$, PDI = 1.6,
- **^{1}H NMR** ($CDCl_3$, ppm), δ: 1.28, 1.85, 3.30-3.98,
- **^{13}C NMR** ($CDCl_3$, ppm), δ: 17, 52, 73, 78,
- **DSC**: T_g = –63 °C.

3 Results and Discussion

3.1 Synthesis of a triblock copolymer of PPG-GAP-PPG

In order to synthesize the triblock copolymer of PPG-GAP-PPG, the first step was the synthesis of GAP with a molecular weight of 1006 $g{\cdot}mol^{-1}$, and this was used as macroinitiator in the preparation of the proposed triblock copolymer (Scheme 1). In fact, a lower molecular weight of the pre-polymer decreases the viscosity and consequently improves its processability. On the other hand, the synthesized triblock copolymer would have primary hydroxyl groups, which in comparison to the secondary ones in GAP, would improve the curing conditions. The triblock copolymer PPG-GAP-PPG was synthesized by cationic ring-opening polymerization of propylene oxide in the presence of $BF_3{\cdot}OEt_2$ as the catalyst.

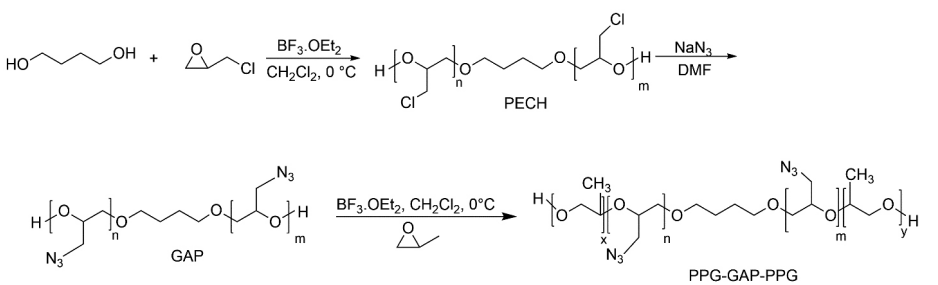

Scheme 1. Synthesis of the triblock copolymer PPG-GAP-PPG

As is shown in Figure 1, the FT-IR spectra of GAP and the synthesized PPG-GAP-PPG triblock copolymer showed characteristic peaks at 3400, 2900, and 2880 cm^{-1} corresponding to –OH group, $–CH_2–$ and C–H asymmetric and symmetric stretching vibrations, respectively. Both spectra showed a peak at 2100 cm^{-1}, which corresponds to the $–N_3$ group in the GAP unit. The C–O–C ether stretching vibration appeared at 1100 cm^{-1}. As can be seen in Figure 1, the triblock copolymer's ether peak is more intense, in comparison to the GAP case, because in the PPG-GAP-PPG triblock copolymer, the number of ether units have been increased.

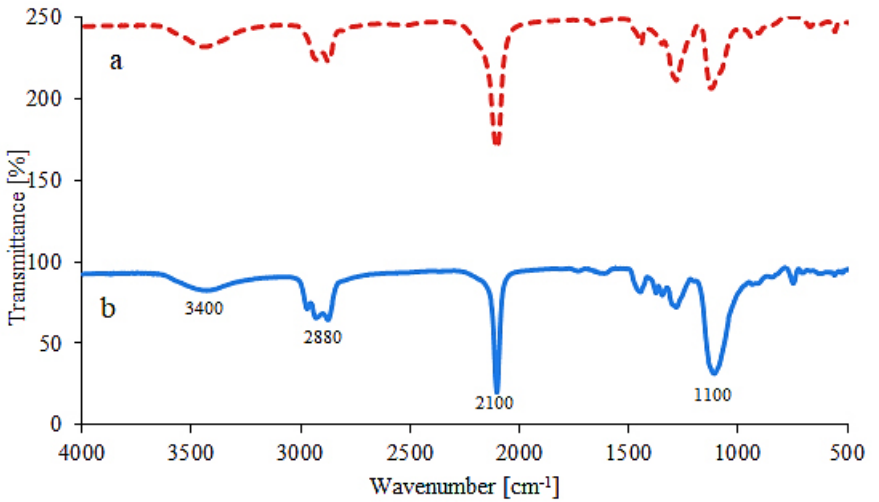

Figure 1. Fourier transform infrared spectrum (FT-IR) of (a) GAP, and (b) the triblock copolymer PPG-GAP-PPG

Figure 2 shows the ^1H NMR spectra of GAP and the PPG-GAP-PPG triblock copolymer. In the case of GAP, the signal at about 1.65 ppm (e) corresponds to methylene protons of the BDO unit. The methylene protons of ($–CH_2–N_3$) appeared at 3.35 ppm. The peaks at 3.58-3.98 ppm are attributed to the methylene protons ($–O–CH_2$). The spectrum of the triblock copolymer PPG-GAP-PPG shows the same characteristic peaks as GAP. The peaks at 1.28 ppm are attributed to the methyl groups ($–CH_3$) in the PPG unit. So the attachment of PPG to GAP is confirmed by the ^1H NMR spectrum. The ^{13}C NMR spectra (Figure 3) exhibited signals at about 17 ($–CH_3$), 52 ($–CH_2N_3$), 73 (C(H)–O) and 78 ($–CH_2O$) ppm [31], again confirming the success of the copolymerization reaction.

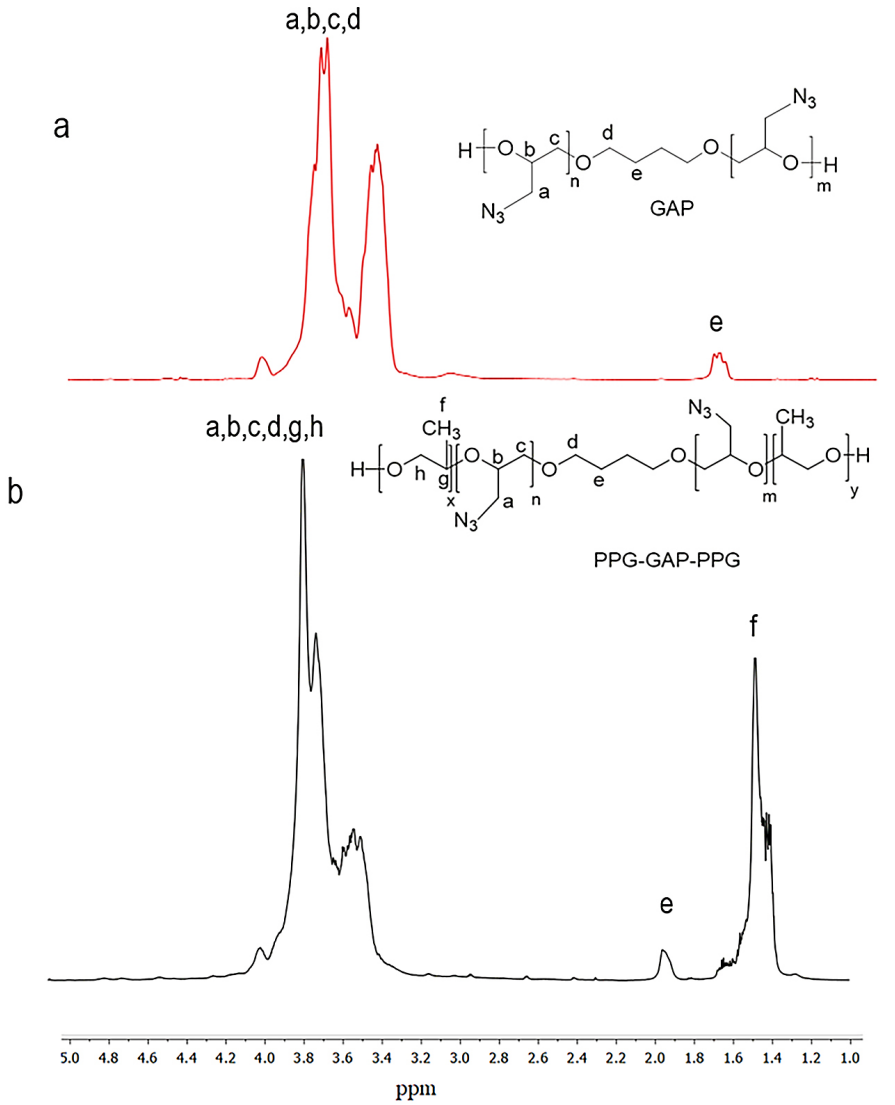

Figure 2. ^{1}H NMR spectrum of (a) GAP and (b) the triblock copolymer PPG-GAP-PPG

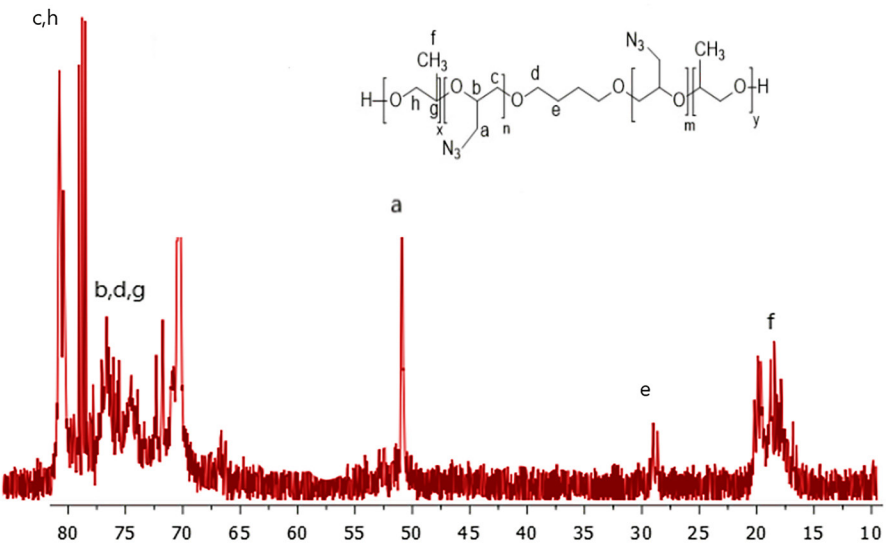

Figure 3. ^{13}C NMR spectrum of the triblock copolymer PPG-GAP-PPG

3.2 Thermal behaviour of the PPG-GAP-PPG triblock copolymer

The investigation of the thermal decomposition behaviour of propellant energetic binders is crucial for evaluating their thermal stability, storage, and processing conditions. A high-temperature DSC thermogram was used for this purpose and the isoconversional methods proposed by Flynn-Wall-Ozawa (FWO) and Kissinger were applied to study the thermal decomposition kinetic factors, such as rate constant, pre-exponential factor (A) and activation energy based on TGA/DSC thermograms using the ASTM method E698 [32, 33].

In the Kissinger method, according to Equations 1 and 2, the activation energy of the decomposition step (E_a) and the pre-exponential factor of the synthesized PPG-GAP-PPG triblock copolymer were calculated at different heating rates (β), 10, 20, 30 and 40 °C·min^{-1}.

$$A = \beta E_a e^{\frac{E_a}{RT}} \Big/ RT^2 \tag{1}$$

$$\ln\left(\frac{\beta}{T_m^2}\right) = \frac{-E_\alpha}{R}\frac{1}{T_m} \tag{2}$$

where β is the heating rate, E_a is the activation energy, and R is the gas constant.

According to Equations 1 and 2, the E_α is obtained from the slope of the plot of $\ln(\beta/(T_m)^2)$ *vs.* $1/T_m$ because this slope is equal to $-E_\alpha/R$.

Equation 3 was used to calculate the activation energy (E_α) by the FWO method for the constant heating rates. In Equation 3, C is a constant, T_α is attributed to the temperature at the selected conversion degree (α), R is the ideal gas constant and β is the heating rate [34-37].

$$log\,\beta = C - \left(0.4567\frac{E_\alpha}{RT_\alpha}\right) \tag{3}$$

The degree of the conversion was calculated by Equation 4:

$$Mass\ (\%)\ = \frac{(m_t - m_f)}{(m_i - m_f)} \tag{4}$$

where m_t is the mass at a certain reaction time t, m_i is the mass at the beginning, and m_f is the mass at the end of the degradation step or steps. The conversion (%) can be calculated by Equation 5.

$$Conversion\ (\%) = 100 - mass \tag{5}$$

3.3 Half-life study

Equations 6 and 7 were used to calculate the rate constant and the half-life of the decomposition reaction by inserting the kinetic parameters E_α and Arrhenius constant (A), and assuming a first-order reaction.

$$k = Aexp^{-\frac{Ea}{RT}} \tag{6}$$

$$t_{1/2} = \frac{0.693}{k} \tag{7}$$

The thermal analyses of GAP and the copolymer were investigated and their T_g values were determined. Figure 4 shows the DSC thermograms of the synthesized GAP with low molecular weight, and the PPG-GAP-PPG triblock, run at 10 °C·min^{-1}. The results for the triblock copolymer showed that it had only one T_g, due to the purity of the synthesized product and the compatibility between the GAP and PPG blocks in the copolymer. The glass transition temperature of PPG-GAP-PPG triblock copolymer

was lower (T_g = −63 °C) than that of the GAP sample (T_g = −53 °C), because of the flexible groups present in the PPG (T_g = −70 °C). This result indicates that the glass transition temperature of GAP has been improved by the copolymerization reaction.

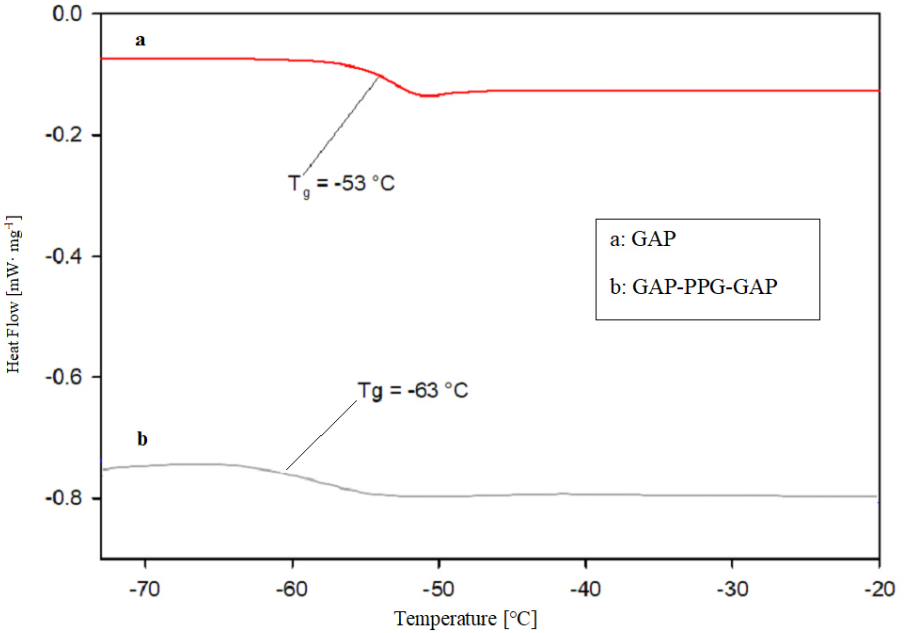

Figure 4. Comparison of the DSC thermograms of the triblock copolymer (PPG-GAP-PPG) and GAP

Figures 5 and 6 show the thermal gravimetric thermogram (TG) and derivative thermo-gravimetric curve (DTG) of the PPG-GAP-PPG triblock copolymer at different heating rates. Two main degradation peaks were observed by DTG. The first step (220-250 °C) is attributed to the exothermic decomposition of the azido group in the sample, whereas the second one, at about 300-320 °C, corresponds to the degradation of the polyether backbone. For GAP, the first decomposition temperature was in the range 202-240 °C and the second step at 260-270 °C. Therefore, the results indicate that the triblock copolymer of PPG-GAP-PPG is more stable than GAP [38].

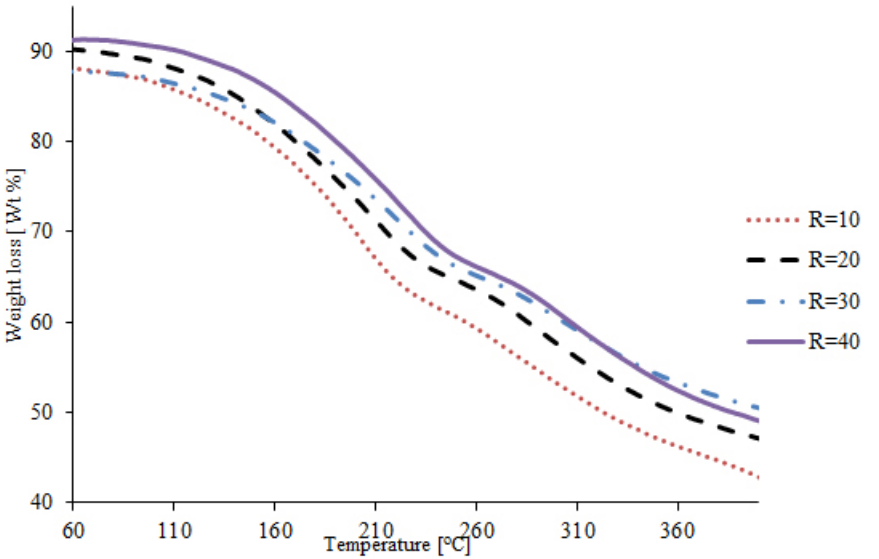

Figure 5. TG thermograms of the PPG-GAP-PPG triblock copolymer at various heating rates (10, 20, 30, and 40 °C·min^{-1})

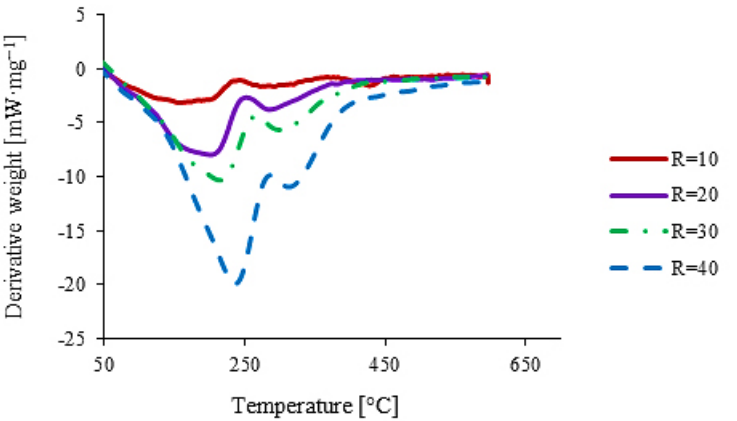

Figure 6. Derivative thermogravimetric curves (DTG) of the PPG-GAP-PPG triblock copolymer at various heating rates (10, 20, 30, and 40 °C·min^{-1})

3.4 Kinetics of thermal decomposition of PPG-GAP-PPG

As can be seen in Figure 7, the Kissinger plot of $\ln(\beta/(T_m)^2)$ *versus* $1/T_m$ is linear, which indicates that the mechanism of thermal decomposition of the triblock copolymer is first order. According to Equation 2, the activation

energies of the first and second steps of the triblock copolymer decomposition were obtained as 215.6 ($R^2 = 0.99$) and 191.22 kJ·mol^{-1} ($R^2 = 0.96$), respectively.

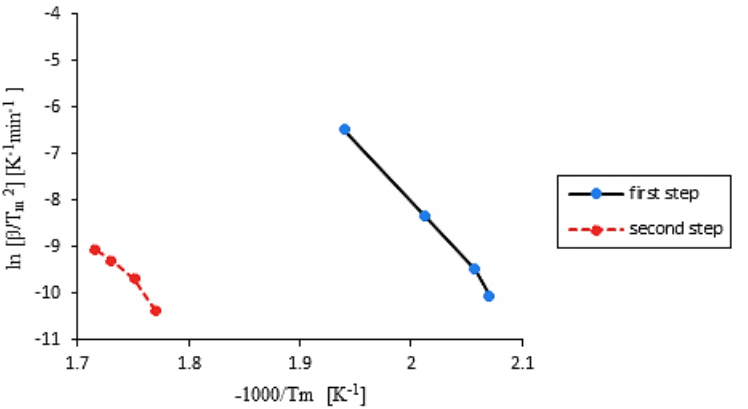

Figure 7. Kissinger plot of $\ln(\beta/(T_m)^2)$ *vs.* $1/T_m$

According to Equation 3 (FWO method), by calculating the slope of the logβ *versus* $1/T$ plot (Figure 8), the E_α of the triblock copolymer was obtained for each degree of degradation (α). The dependence of E_α on percentage conversion, calculated by the FWO and Kissinger methods can be seen in Figure 9. It can be found that the results of these two methods were similar. In the FWO method, E_α increased up to 60% conversion, and then decreased. The range of E_α was 180.52-359 kJ·mol^{-1} up to 60% conversion. The plots showed that in the conversion of about 30%, the value of E_α was the same for two methods. According to the ASTM method E698, DSC data (Figure 10) were applied to evaluate the thermokinetic parameters corresponding to the thermal decomposition of the copolymer.

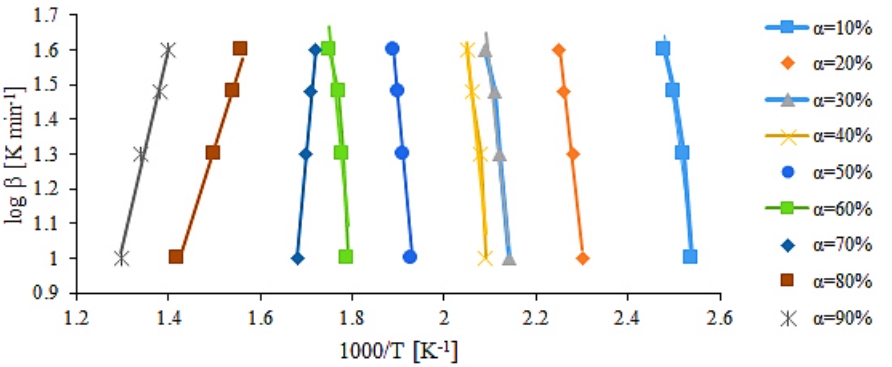

Figure 8. Plots of logβ *vs.* $1/T$ for the FWO method

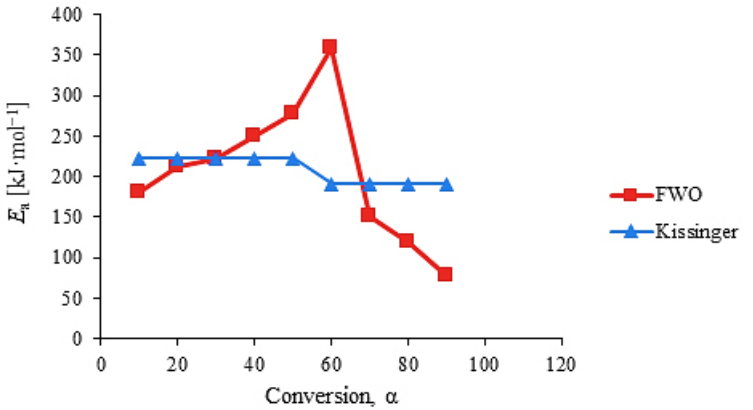

Figure 9. Dependence of the activation energy on the percentage conversion

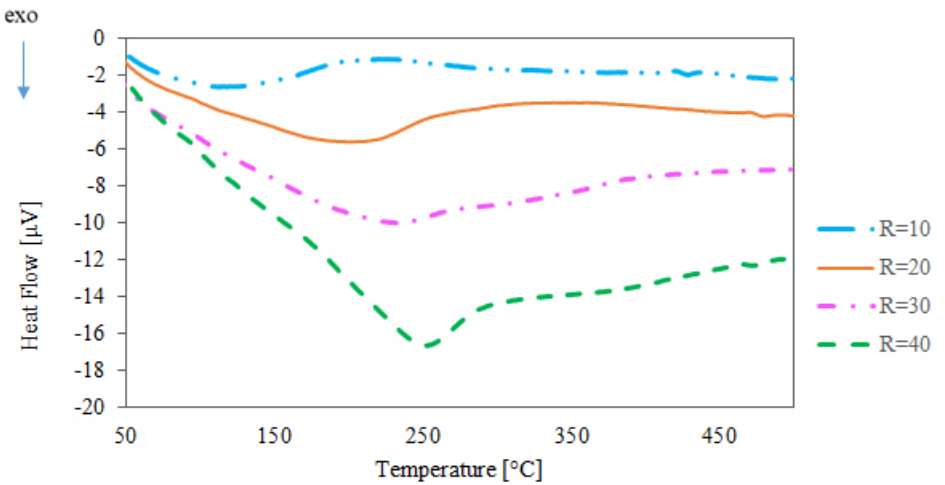

Figure 10. DSC thermogram of PPG-GAP-PPG samples at various heating rates (10, 20, 30 and 40 °C·min^{-1})

As shown in Figure 11, a plot of logarithm of the heating rate *versus* the reciprocal of the peak absolute temperature for the triblock copolymer was linear, with $R^2 = 0.9908$. Figure 12 also indicated that the mechanism of the thermal decomposition of the triblock copolymer was first order, because the plot of $\ln(\beta/T^2)$ *vs.* $1/T_p$ was linear [39]. Based on Equations 1 and 2, the ASTM method E698 was used to calculate the activation energy (slope of the $\ln(\beta/T^2)$ *vs.* $1/T_p$) and the pre-exponential factor (Table 1).

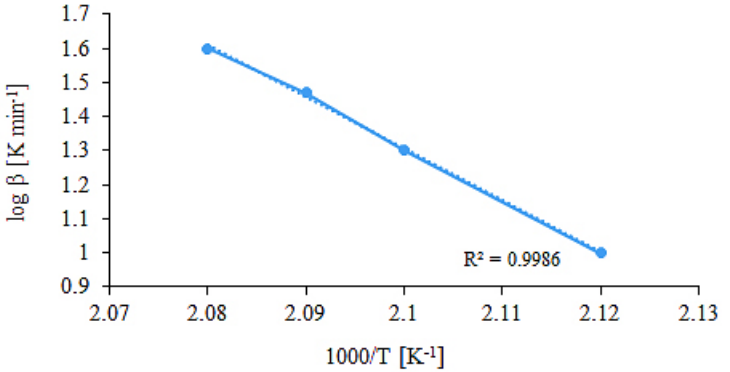

Figure 11. Plot of logβ *vs.* 1/T

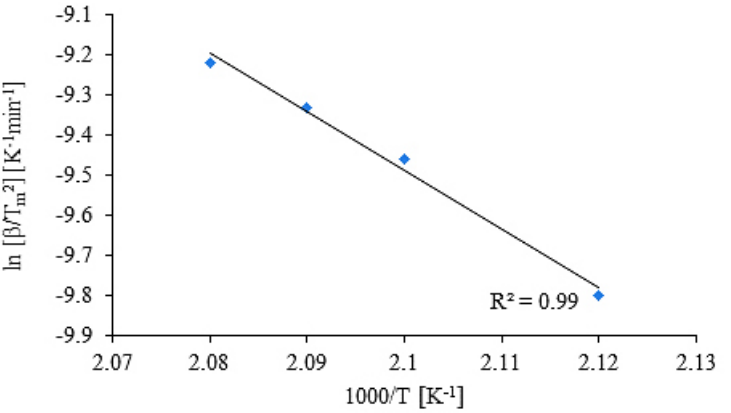

Figure 12. Plot of ln(β/T$^{2)}$ vs. 1/T

Table 1. Comparison of the kinetic parameters for the triblock copolymer, obtained by the ASTM and FWO methods

Method	E_a [kJ·mol^{-1}]	log$A$ [min^{-1}]	k	R^2	Half-life $t_{1/2}$ [year]
ASTM	126.13	13.93	$3.5 \cdot 10^{-7}$	0.9986	3.76
FWO	124.610	13.76	$4.140 \cdot 10^{-7}$	0.9938	3.18

3.5 Half-life determination

Based on the resulting kinetic parameters (E_a and A) and assuming first-order decomposition, the half-life ($t_{1/2}$) and the reaction rate constant (k) were calculated using Equations 6 and 7 at 50 °C. Table 1 shows a comparison

of the kinetic parameters for the triblock copolymer obtained by the ASTM and FWO methods

4 Conclusions

An energetic triblock copolymer PPG-GAP-PPG was successfully synthesized by cationic ring-opening polymerization of propylene oxide and glycidyl azide polymer as macroinitiator, in the presence of $BF_3 \cdot OEt_2$ as catalyst. The thermal behaviour of the synthesized novel energetic binder (PPG-GAP-PPG) was investigated by TG, DSC, DTG thermograms for the first time. The synthesized triblock copolymer with a PPG content of about 45% has a glass transition temperature of −63 °C, which indicates that has better thermal properties than GAP ($T_g = -53$ °C).

The synthesized triblock copolymer PPG-GAP-PPG was more stable than GAP due to its higher decomposition temperature. The kinetic parameters, such as activation energy and frequency factor, for the thermal decomposition of the triblock copolymer PPG-GAP-PPG were obtained from the DSC and DTG data by the non-isothermal methods proposed by ASTM E698, Flynn-Wall-Ozawa (FWO) and Kissinger. The values obtained by the FWO and ASTM methods were in good agreement with each other. The half-life of the triblock copolymer at 50 °C was estimated to be about 3 years.

References

[1] Badgujar, D.; Talawar, M.; Asthana, S.; Mahulikar, P. Advances in Science and Technology of Modern Energetic Materials: An Overview. *J. Hazard Mater.* **2008**, *151*(2-3): 289-305.

[2] Mahkam, M.; Nabati, M.; Latifpour, A.; Aboudi, J. Synthesis and Characterization of New Nitrogen-rich Polymers as Candidates for Energetic Applications. *Des. Monomers Polym*. **2014**, *17*(5): 453-457.

[3] Abrishami, F.; Zohari, N.; Zeynali, V. Synthesis and Kinetic Study on the Thermal Degradation of Triblock Copolymer of Polycaprolactone-Poly(Glycidyl Nitrate)-Polycaprolactone (PCL-PGN-PCL) as an Energetic Binder. *Polym. Adv. Technol*. **2019**;*30*(3):640-647

[4] Betzler, F.M.; Hartdegen, V.A.; Klapötke, T.M.; Sproll, S.M. A New Energetic Binder: Glycidyl Nitramine Polymer. *Cent. Eur. J. Energ. Mater*. **2016**, *13*(2): 289-300.

[5] Ampleman, G. *Glycidyl Azide Polymer.* US Patent 5359012, **1994**.

[6] Selim, K.; Özkar, S.; Yilmaz, L. Thermal Characterization of Glycidyl Azide Polymer (GAP) and GAP-based Binders for Composite Propellants. *J. Appl. Polym. Sci*. **2000**, *77*(3): 538-546.
[7] *Chemical Rocket Propulsion: A Comprehensive Survey of Energetic Materials.* (DeLuca, L.T.; Shimada, T.; Sinditskii, V.P.; Calabro, M., Eds.) Springer, **2017**; ISBN 978-3-319-27746-2.
[8] Pisharath, S.; Ang, H.G. Thermal Decomposition Kinetics of a Mixture of Energetic Polymer and Nitramine Oxidizer. *Thermochim. Acta* **2007**, *459*(1-2): 26-33.
[9] Gaur, B.; Lochab, B.; Choudhary, V.; Varma, I. Azido Polymers – Energetic Binders for Solid Rocket Propellants. *J. Macromol. Sci., C Polymer Rev*. **2003**, *43*(4): 505-545.
[10] Meyer, R.; Köhler, J.; Homburg, A. *Explosives.* John Wiley & Sons, **2016**.
[11] Wang, X.; Shu, Y.; Lu, X.; Mo, H.; Xu, M. Synthesis and Characterization of PolyNIMMO-HTPB-PolyNIMMO Triblock Copolymer as a Potential Energetic Binder. *Cent. Eur. J. Energ. Mater*. **2018**, *15*(3): 456-467.
[12] Bayat, Y.; Chizari, M. Synthesis, Characterization and Stability of Triblock Copolymer Based on Tetrahydrofuran and Glycidylazide as Binder. *Polym. Sci. Ser. B.* **2018**, *60*(5): 621-628.
[13] Chizari, M.; Bayat, Y. Synthesis and Kinetic Study of a PCL-GAP-PCL Tri-block Copolymer. *Cent. Eur. J. Energ. Mater*. **2018**, *15*(2): 243-257.
[14] Sun, M.B. Characterization of the Plasticized GAP/PEG and GAP/PCL Block Copolyurethane Binder Matrices and Its Propellants. *Propellants, Explos., Pyrotech.* **2008**, *33*(2): 131-138.
[15] Min, B.S.; Ko, S.W. Characterization of Segmented Block Copolyurethane Network Based on Glycidyl Azide Polymer and Polycaprolactone. *Macromol. Res.* **2007**, *15*(3): 225-233.
[16] Deng, J.; Li, G.; Xia, M.; Lan, Y.; Luo, Y. Improvement of Mechanical Characteristics of Glycidyl Azide Polymer Binder System by Addition of Flexible Polyether. *J. Appl. Polym. Sci.* **2016**, *133*(35): 43840-43847.
[17] Vasudevan, V.; Sundararajan, G. Synthesis of GAP-PB-GAP Triblock Copolymer and Application as Modifier in AP/HTPB Composite Propellant. *Propellants, Explos., Pyrotech.* **1999**, *24*(5): 295-300.
[18] Mathew, S.; Manu, S.K.; Varghese, T.L. Thermomechanical and Morphological Characteristics of Cross-linked GAP and GAP-HTPB Networks with Different Diisocyanates. *Propellants, Explos., Pyrotech.* **2008**, *33*(2): 146-152.
[19] Pisharath, S.; Ang, H.G. Synthesis and Thermal Decomposition of GAP-Poly(BAMO) Copolymer. *Polym. Degrad. Stab.* **2007**, *92*(7): 1365-1377.
[20] Soman, R.; Athar, J.; Agawane, N.; Shee, S.; Gore, G.; Sikder, A. Synthesis, Characterization and Rheology of Tetrafunctional Glycidyl Azide Polymer vis-à-vis Difunctional GAP. *Polym. Bull.* **2016**, *73*(2): 449-461.
[21] Ertem, S.P.; Yilgor, E.; Kosak, C.; Wilkes, G.L.; Zhang, M.; Yilgor, I. Effect of Soft Segment Molecular Weight on Tensile Properties of Poly(propylene oxide) Based Polyurethaneureas. *Polymer* **2012**, *53*(21): 4614-4622.

[22] Herzberger, J.; Niederer, K.; Pohlit, H.; Seiwert, J.; Worm, M.; Wurm, F.R.; Frey, H. Polymerization of Ethylene Oxide, Propylene Oxide, and other Alkylene Oxides: Synthesis, Novel Polymer Architectures, and Bioconjugation. *Chem. Rev.* **2015**, *116*(4): 2170-2243.

[23[Johari, G.; Hallbrucker, A.; Mayer, E. Calorimetric Relaxation and Glass Transition in Poly(propylene glycols) and Its Monomer. *J. Polym. Sci., B: Polymer Physics* **1988**, *26*(9): 1923-1930.

[24] Lindner, R.; Lejkowski, M.L.; Lavy, S.; Deglmann, P.; Wiss, K.T.; Zarbakhsh, S.; Meyer, L.; Limbach, M. Ring-opening Polymerization and Copolymerization of Propylene Oxide Catalyzed by *N*-Heterocyclic Carbenes. *ChemCatChem*. **2014**, *6*(2): 618-625.

[25] Furukawa, M.; Yokoyama, T. Mechanical Properties of Organic-Inorganic Polyurethane Elastomers. I. $Al(OH)_3$-Polyurethane Composites Based on PPG. *J. Appl. Polym. Sci.* **1994**, *53*(13): 1723-1729.

[26] Cooper, W.; Pope, G.; Vaughan, G. Polypropylene Oxide Elastomers-I. Polymer Synthesis and Vulcanization. *Eur. Polym. J.* **1968**, *4*(2): 207-216.

[27] Barlow, A.J.; Erginsav, A. Viscoelastic Properties of Poly(propylene glycols). *Polymer* **1975**, *16*(2): 110-114.

[28] Min, B.S. Synthesis of Azide-terminated Glycidyl Azide Polymer with Low Molecular Weight. *J. Korea Inst. Mil. Sci. Technol*. **2005**, *8*(1): 69-80.

[29] Kubota, N.; Sonobe, T. Combustion Mechanism of Azide Polymer. *Propellants, Explos., Pyrotech.* **1988**, *13*(6): 172-177.

[30] Holden, G. *Understanding Thermoplastic Elastomers.* Hanser Verlag, **2000**; ISBN 978-1569902899.

[31] Uyar, T.; Hacaloğlu, J. Thermal Degradation of Poly(propylene oxide) and Polyepichlorohydrin by Direct Pyrolysis Mass Spectrometry. *J. Anal. Appl. Pyrolysis*. **2002**, *64*(2): 379-393.

[32] Sivalingam, G.; De, P.; Karthik, R.; Madras, G. Thermal Degradation Kinetics of Vinyl Polyperoxide Copolymers. *Polym. Degrad. Stab*. **2004**, *84*(1): 173-179.

[33] Ries, A.; Canedo, E.L.; Souto, C.R.; Wellen, R.M. Non-isothermal Cold Crystallization Kinetics of Poly(3-hydoxybutyrate) Filled with Zinc Oxide. *Thermochim. Acta* **2016**, 637: 74-81.

[34] Singh, A.; Sharma, T.C.; Kumar, M.; Narang, J.K.; Kishore, P.; Srivastava, A. Thermal Decomposition and Kinetics of Plastic Bonded Explosives Based on Mixture of HMX and TATB with Polymer Matrices. *Def. Technol.* **2017**, *13*(1): 22-32.

[35] Li, H.; Pan, R.; Wang, W.; Zhang, L. Thermal Decomposition and Kinetics Studies on Poly(BDFAO/THF), Poly(DFAMO/THF), and Poly(BDFAO/DFAMO/THF). *J. Therm. Anal. Calorim*. **2014**, *118*(1): 189-196.

[36] Liu, S.J.; Hou, X.; Fang, C.G.; Ma, R.T.; Jiang, Z.H. Thermal Degradation Kinetics and Lifetime Prediction of Poly(aryl ether ketone)s containing 2,6-Naphthalene Moieties. *J. Appl. Polym. Sci*. **2009**, *112*(2): 904-909.

[37] ASTM E698-05 *Standard Test Method for Arrhenius Kinetic Constants for*

Thermally Unstable Materials Using Differential Scanning Calorimetry and the Flynn/Wall/Ozawa Method. **2005**.

[38] Kishore, K.; Sridhara, K. *Solid Propellant Chemistry Condensed Phase Behaviour of Ammonium Perchlorate-based Solid Propellants*. DESIDOC, Dehli, **1999**, p. 149; ISBN 81-86514-02-6.

[39] Sunitha, M.; Nair, C.R.; Krishnan, K.; Ninan, K. Kinetics of Alder-ene Reaction of Tris(2-allylphenoxy)triphenoxycyclotriphosphazene and Bismaleimides – a DSC Study. *Thermochim. Acta* **2001**, *374*(2): 159-169.

Received: July 4, 2019
Revised: June 19, 2020
First published online: June 25, 2020